



CrossMark
click for updates

Cite this: *RSC Adv.*, 2016, 6, 19233

Received 8th January 2016
Accepted 2nd February 2016

DOI: 10.1039/c6ra00648e

www.rsc.org/advances

Stability of Li_2CO_3 in cathode of lithium ion battery and its influence on electrochemical performance

Yujing Bi,^{abd} Tao Wang,^c Meng Liu,^a Rui Du,^{ab} Wenchao Yang,^a Zixuan Liu,^a Zhe Peng,^a Yang Liu,^a Deyu Wang^{*a} and Xueliang Sun^d

Lithium carbonate is an unavoidable impurity at the cathode side. It can react with LiPF_6 -based electrolyte and LiPF_6 powder to produce LiF and CO_2 , although it presents excellent electrochemical inertness. Samples of Li_2CO_3 -coated and LiF -coated $\text{LiNi}_{0.8}\text{Co}_{0.1}\text{Mn}_{0.1}\text{O}_2$ were prepared to compare their influence on a cathode's behavior. After 200 cycles at 1C, in contrast to 37.1% of capacity retention for the Li_2CO_3 -coated material, the LiF -coated $\text{LiNi}_{0.8}\text{Co}_{0.1}\text{Mn}_{0.1}\text{O}_2$ retained 91.9% of its initial capacity, which is similar to the fresh sample. This demonstrates that decomposition of Li_2CO_3 can seriously deteriorate cyclic stability if this occurs during working.

Introduction

Lithium ion batteries (LIB) are the most successful electrochemical energy storage technology of recent decades. As a chemical system, the performance of LIB is influenced by impurities, including species introduced by the components or *in situ* generated during working.^{1–5} A good understanding of their chemical behavior and influence on cell performance is important in development of high-quality commercial batteries.

At the cathode side, impurities of lithium carbonate are unavoidable because of the carbonate-based electrolyte and the meta-stability of cathode materials.^{6–9} Li_2CO_3 has good electrochemical inertness, thus it is considered as a suitable component for construction of the cathode's protective layer.^{10–12} However, its appearance is often accompanied by serious capacity fading of cathode materials, especially for nickel rich layer oxides.^{13–16} To the authors' knowledge, this contradiction in the role of lithium carbonate has not been carefully investigated to date.

Here we research the stability of lithium carbonate on the cathode side, and its influence on electrochemical performance

of $\text{LiNi}_{0.8}\text{Mn}_{0.1}\text{Co}_{0.1}\text{O}_2$. Although it possesses excellent electrochemical inertness, the exposed Li_2CO_3 particles react easily with LiPF_6 -based electrolyte and LiPF_6 powder to generate LiF , CO_2 , and POF_3 . For a comparison, samples of Li_2CO_3 -coated and LiF -coated $\text{LiNi}_{0.8}\text{Co}_{0.1}\text{Mn}_{0.1}\text{O}_2$ were prepared. In contrast to the poor cyclic stability of Li_2CO_3 -coated material, LiF -coated samples present much better cyclic stability, which is similar to the fresh pristine material.

Experimental section

LiPF_6 (Kanto Chemical Co., Inc., 99%), LiTFSI (MMM, Ltd, 98%), and Li_2CO_3 (Aladin, >99%) were dried at 120 °C under vacuum in a transfer chamber of an Ar-glove box for 48 h before use. An electrolyte of 1 mol L^{-1} LiPF_6 dissolved in mixed solution of propyl carbonate (PC) and dimethyl carbonate (DMC) (1 : 1, v/v) (Guotai Huarong Chemical New Material Co., Ltd) was used as received.

The chemical stability of Li_2CO_3 was evaluated by immersing the powder material (1 g) in 5 mL electrolyte, sealing in Al-plastic packages, and then heating at 30 °C, 55 °C, 80 °C, and 100 °C for 12 h in an Ar-glove box. Powders of Li_2CO_3 (0.49 g) and LiPF_6 (2 g) were also mixed and sealed in Al-plastic packages to heat at 80 °C for 12 h. To check the interactions between water and LiPF_6 , 10 mL H_2O was slowly dropped onto 2 g LiPF_6 powder. Moreover, 2 g LiPF_6 powder was fast dissolved into 10 mL H_2O .

$\text{LiNi}_{0.8}\text{Co}_{0.1}\text{Mn}_{0.1}\text{O}_2$ was synthesized by the high-temperature solid-state method as published.^{16,17} The Li_2CO_3 -coated $\text{LiNi}_{0.8}\text{Co}_{0.1}\text{Mn}_{0.1}\text{O}_2$ was obtained by storing $\text{LiNi}_{0.8}\text{Co}_{0.1}\text{Mn}_{0.1}\text{O}_2$ at 55 °C with saturated steam (15 kPa) in a desiccator for 1 month. The LiF -coated $\text{LiNi}_{0.8}\text{Co}_{0.1}\text{Mn}_{0.1}\text{O}_2$ was prepared by immersing the Li_2CO_3 -coated sample in electrolyte and heating at 80 °C for 12 h.

The electrode was composed of cathode material, super P and polyvinylidene fluoride (PVdF) at weight ratio 8 : 1 : 1 suspended in NMP, and the slurry was casted on aluminum foil current collectors. The electrode was dried at 120 °C under

^aNingbo Institute of Materials Technology and Engineering, Chinese Academy of Sciences, Ningbo, 315201, China. E-mail: wangdy@nimte.ac.cn

^bUniversity of Chinese Academy of Sciences, Beijing, 100049, China

^cShanghai Institute of Space Power Source, Shanghai, 200245, China

^dNanomaterial and Energy Lab, Department of Mechanical and Materials Engineering, University of Western Ontario, London, Ontario, N6A 5B9, Canada

a vacuum for 12 h and then punched into ϕ 16 mm disks. CR2032 coin cells were assembled with the prepared electrode as cathode, lithium foil as anode, Celgard 2550® as separator, and 1 mol L⁻¹ LiPF₆ in a mixture solution of polycarbonate (PC)/dimethyl carbonate (DMC) (1 : 1, v/v) as the electrolyte. Cell assembly was performed in an Ar-filled M-Braun glove box, in which H₂O and O₂ were controlled less than 1 ppm. Linear sweep voltammetry between 2.5 and 5.5 V vs. Li/Li⁺ at 0.1 mV s⁻¹ rate was carried out at an electrochemical work station (Solartron, 1470E). Electrochemical measurements were performed on a battery tester of Land 2001A (Wuhan, China) between 2.8 and 4.3 V vs. Li/Li⁺ at 25 °C at various rates.

The powders were characterized by X-ray diffraction with a Bruker D8 advanced diffractometer using CuK α ($\lambda = 1.5406$ Å) radiation (Bruker AXS, D8 Advance) between 10° and 60° by 0.02° steps. Analysis of microscopy was performed by scanning electron microscopy (SEM, Hitachi, S4800) and transmission electron microscopy (TEM, FEI, Tecnai F20, 200 kV). Surface analysis was conducted with a PHI 3056 X-ray photoelectron spectrometer (XPS), which was excited by Mg K α radiation at a constant power of 100 W (15 kV and 6.67 mA). The gas species were analyzed on a gas chromatograph mass spectrometer (GC-MS, Agilent 7890B-5977A, EI). The column of GC is a capillary column chromatograph (Agilent, HP-PLOT/U).

Results and discussion

The purchased lithium carbonate could be attributed to the *C2/c* space group of monoclinic system with particle size at 2–10 μ m, as shown in Fig. 1a. This has good electrochemical inertness, with decomposition reaction peaking at \sim 5.3 V vs. Li/Li⁺ as shown in Fig. 1b. Clearly, Li₂CO₃ is electrochemically stable inside the lithium ion cells at current working conditions.

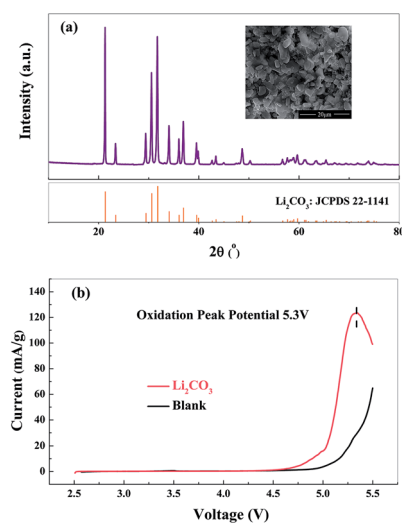


Fig. 1 Characterization of commercial Li₂CO₃ powder: (a) XRD pattern and SEM image; (b) linear sweep voltammetry with Li₂CO₃ electrode as working electrode, Li foil as counter and reference electrode, and scanned with 0.1 mV s⁻¹.

The chemical stability of Li₂CO₃ was evaluated *via* experiment with a mixture of 1 g Li₂CO₃ and 5 mL electrolyte sealed in an Al-plastic package and heated at 30 °C, 55 °C, 80 °C, 100 °C. When treated at 30 °C, the signal of Li₂CO₃ is gradually weakened over time, as shown in Fig. 2a. In contrast, LiF peaks are detectable after 2 days of storage, and their intensities are strengthened after 30 days. As the temperature increases to 55 °C, lithium fluoride is one of the dominant phases after 12 h heat treatment. In the sample treated at 80 °C and 100 °C after 12 h, LiF becomes the single crystalline phase (Fig. 2b). This indicates that Li₂CO₃ should react chemically with LiPF₆ to generate lithium fluoride as the solid product.

The generated gas in the package is tested by GC-MS. In all tested packages, CO₂ and POF₃ are the extremely dominant gaseous species, with a ratio more than 90%, as demonstrated

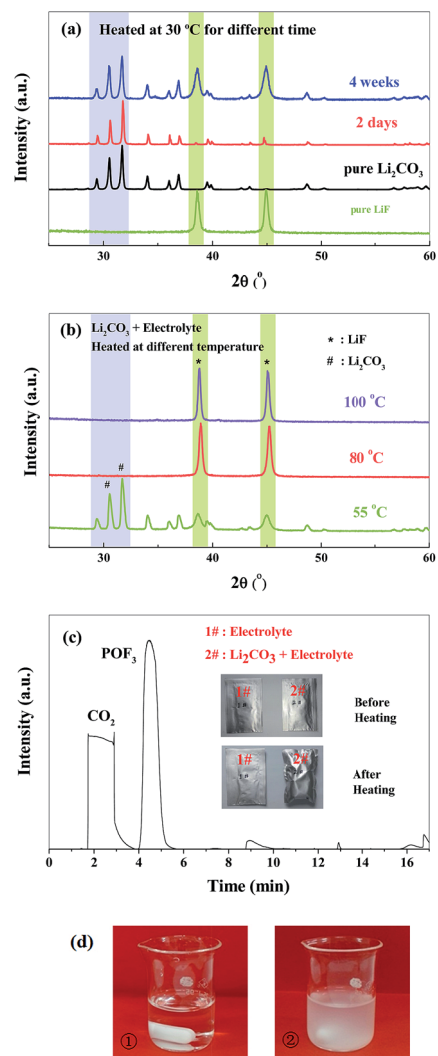
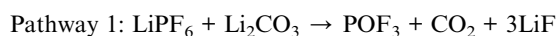


Fig. 2 (a) XRD pattern comparison of Li₂CO₃ immersed in electrolyte at 30 °C for 2 days and 4 weeks; (b) XRD pattern comparison of Li₂CO₃ heating in electrolyte at 55 °C, 80 °C, and 100 °C for 12 h; (c) GC-MS results and digital pictures of Al-plastic package before and after heating (1#, 2#); (d) digital pictures of LiPF₆ crystal dissolved by different ways (① LiPF₆ powder is fast dissolved into water, ② water is slowly dropped onto LiPF₆ crystal).

in Fig. 2c. Carbon dioxide could be decomposed from Li_2CO_3 , and POF_3 could be attributed to reaction of the PF_6^- group with a trace amount of moisture.¹⁸ Small chromatographic peaks at 9, 13, and 16.2 min would be caused by corrosion of HF. Combined with the XRD results, lithium carbonate should be reacted spontaneously with electrolyte to generate LiF as the solid product, and CO_2 and POF_3 as the gaseous species.

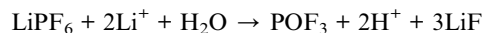
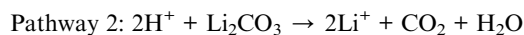
To further explore the probable reason for this reaction, a mixture of Li_2CO_3 and LiPF_6 (1 : 1 in mole) powder was sealed and heated at 80 °C for 12 h. The tested pack ages were inflated quickly. The solid remnant is LiF and the dominant gaseous products are POF_3 and CO_2 , indicating the reaction between solids is the same as for Li_2CO_3 with electrolyte. This result indicates that the Li_2CO_3 decomposition could be preceded by direct attack of LiPF_6 without the assistance of moisture, as shown in Pathway 1, because both salts were thoroughly dried before the test.



According to the LiPF_6 production procedure, it should contain trace amount of HF,¹⁹ which could react with lithium carbonate to produce water. Although PF_6^- groups can react with water in organic media, they are also quite stable in aqueous solution, e.g., NaPF_6 aqueous solution is used as the source of PF_6^- in synthesis of ionic liquids.²⁰ The stability of LiPF_6 powder with a small amount of water, the situation in this case, has not been discussed to the authors' knowledge.

Here dissolution behavior of LiPF_6 salt (2 g) in water (10 mL) was compared with experiments of quickly pouring LiPF_6 powder into water and slowly dropping water into LiPF_6 powder. In the first case, a clear solution was formed with a pH value of ~5, as shown in Fig. 2d1. In the second case, smoke was released when water encountered LiPF_6 powder. After dropping, the solution still contains some insoluble material, as demonstrated in Fig. 2d2, which is lithium fluoride, as identified by XRD. The pH value of the solution is ~2, indicating that H^+ was

generated during dissolving. This demonstrates that LiPF_6 tends to decompose with a small amount of H_2O to generate H^+ . The probable reason for this phenomenon is that PF_6^- ion group could not form a stable hydration layer with the small amount of H_2O .^{21–24} Therefore, a trace amount of HF may catalyze decomposition of lithium carbonate with H^+ as the catalyst, as shown in Pathway 2. This mechanism is possible, although we tend to believe Pathway 1 is more likely.



The chemical stability of Li_2CO_3 with LiTFSI electrolyte and LiTFSI powder was also evaluated to compare the influence of cations. No obvious inflation was observed after storing at 80 °C for 12 h, indicating that Li_2CO_3 decomposition could be related to the PF_6^- group. As no candidate exhibits the possibility of totally replacing LiPF_6 in commercial systems, chemical decomposition of lithium carbonate appears unavoidable when directly exposed to electrolyte. A good understanding of its influence on cathode's performance would be helpful in construction of high-quality cells. As Li_2CO_3 is relatively easy to generate on the surface of nickel-rich content cathodes, $\text{LiNi}_{0.8}\text{Co}_{0.1}\text{Mn}_{0.1}\text{O}_2$ was selected as the target to prepare Li_2CO_3 -coated and LiF-coated samples in the following comparison.

To accelerate the Li_2CO_3 generation rate, a $\text{LiNi}_{0.8}\text{Co}_{0.1}\text{Mn}_{0.1}\text{O}_2$ sample was placed in a glass dish and stored in a desiccator with water at 55 °C for 1 month. The glass jar was opened daily to ensure the CO_2 content. As shown in Fig. 3a and b, the signal of Li_2CO_3 was detected with XRD and XPS after humidity corrosion. And TEM identified the decomposing layer with a thickness of ~18 nm in Fig. 3g. This demonstrates that the sample after humidity corrosion is Li_2CO_3 -coated $\text{LiNi}_{0.8}\text{Co}_{0.1}\text{Mn}_{0.1}\text{O}_2$.

According to the previous results, the Li_2CO_3 -coated sample was mixed with electrolyte and heated at 80 °C for 12 h to prepare a LiF-coated sample. As shown in Fig. 3a, Li_2CO_3 totally

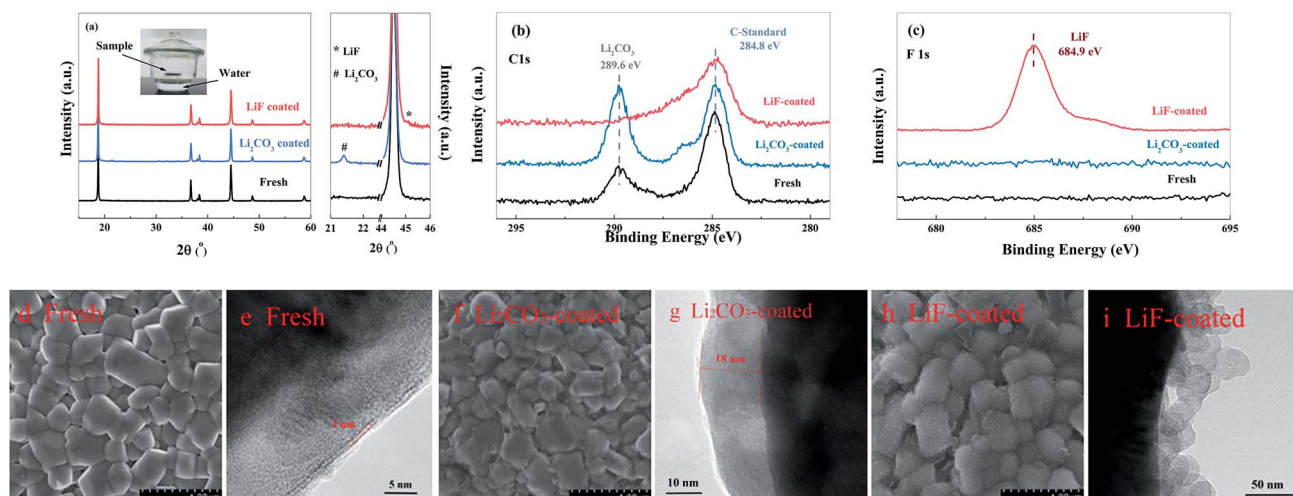
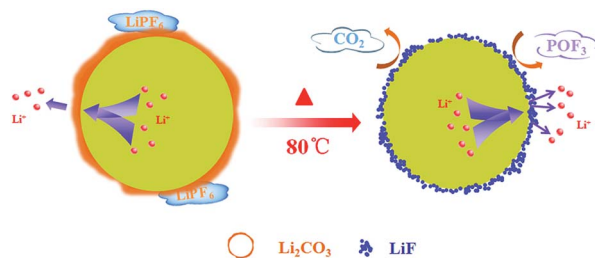


Fig. 3 (a) XRD patterns and C 1s, (b) and F 1s; (c) XPS spectrum of fresh, Li_2CO_3 -coated and LiF-coated $\text{LiNi}_{0.8}\text{Co}_{0.1}\text{Mn}_{0.1}\text{O}_2$ cathode material; SEM and HRTEM images of (d), (e) fresh; (f), (g) Li_2CO_3 -coated; and (h), (i) LiF-coated material.

disappeared, and LiF became the only detectable impurity after this treatment. The weak broadened peak from 687.5 to 689.0 eV in Fig. 3c may be attributed to $\text{Li}_x\text{PO}_y\text{F}_z$ during the heat process in the electrolyte.²⁵ From the TEM images (Fig. 3g and i), it can be seen that the dense Li_2CO_3 layer changes to the porous LiF membrane. These results indicate that LiF-coated $\text{LiNi}_{0.8}\text{Co}_{0.1}\text{Mn}_{0.1}\text{O}_2$ was obtained after the electrolyte attack, which is consistent with the previous results (Scheme 1).

The electrochemical performances of the as-synthesized, Li_2CO_3 -coated and LiF-coated $\text{LiNi}_{0.8}\text{Co}_{0.1}\text{Mn}_{0.1}\text{O}_2$ were



Scheme 1 Surface reaction of Li_2CO_3 -coated material in LiPF_6 electrolyte.

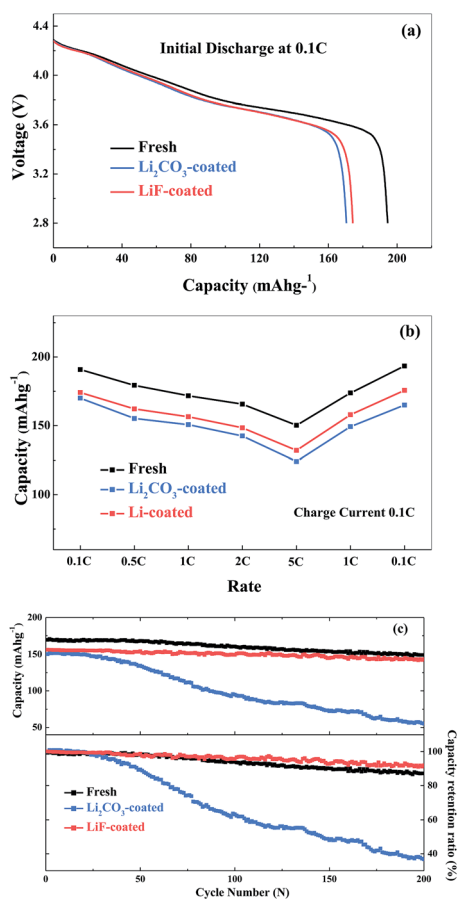


Fig. 4 Electrochemical property of fresh, Li_2CO_3 -coated and LiF-coated $\text{LiNi}_{0.8}\text{Co}_{0.1}\text{Mn}_{0.1}\text{O}_2$ cathode material. (a) The discharge curves in the first cycle at 0.1C; (b) rate capability at 0.1C, 0.2C, 0.5C, 1C, 2C, and 5C; (c) cyclic stability tested at 1C.

compared, as shown in Fig. 4. The discharge capacity of the fresh sample was $192.5 \text{ mA h g}^{-1}$. The discharge capacity of Li_2CO_3 -coated sample dropped to $170.5 \text{ mA h g}^{-1}$ (Fig. 4a). As the discharge plateau is almost overlapped at the initial part, the lost capacity should correspond to the loss of active material rather than polarization. With this hypothesis, the decomposition ratio should be $\sim 12\%$. After the electrolyte attack, sample capacity recuperated to $174.2 \text{ mA h g}^{-1}$. This is probably related to the relatively low molecular weight of lithium fluoride. The rate performance shows the same trend, as shown in Fig. 4b. The fresh, Li_2CO_3 -coated, and LiF-coated samples deliver 150.3, 124.1, and $132.0 \text{ mA h g}^{-1}$ at 5C, respectively.

All samples were cycled under 1C rate, their results are compared in Fig. 4c. The fresh material maintains $149.1 \text{ mA h g}^{-1}$, 87.2% of the initial capacity after 200 cycling. The discharge capacity of the Li_2CO_3 -coated sample seriously fades, only 37.1% is retained after the 200th cycle. In contrast, the LiF-coated sample still presents $143.5 \text{ mA h g}^{-1}$, namely 91.9% of the initial discharge capacity, in the 200th cycle.

This improvement on cyclic stability for LiF-coated $\text{LiNi}_{0.8}\text{Co}_{0.1}\text{Mn}_{0.1}\text{O}_2$ is related to the reaction of Li_2CO_3 decomposition. According to the results in the former part, if reacted inside the cell, the gaseous species of Li_2CO_3 decomposition should be adsorbed on the surface of the cathode material. Gas adsorption decreases the active surface area and gradually aggregates the cell's polarization. A similar phenomenon is observed on a zinc electrode, where the over-potential is quickly augmented by H_2 absorption.^{26,27} As for the LiF-coated sample, the interface between cathode and electrolyte is not affected by the generated gas, therefore it presents cyclic stability.

Conclusion

The role of Li_2CO_3 in LiPF_6 electrolyte was investigated in this study. Although it is electrochemically stable, Li_2CO_3 can be chemically decomposed to LiF as a solid product, CO_2 and POF_3 as gaseous species. The generated gaseous species can be absorbed on the cathode surface, causing aggregation of discharge polarization and deteriorating cyclic stability. As Li_2CO_3 impurity cannot be well controlled in practical production, treatment at high temperature to release the gas should be very helpful to maintain the cell's cyclic stability.

Acknowledgements

We thank the 863 project (Grant No. 2013AA050906), the National Natural Science Foundation of China (Grant No. 51572273), Hundred Talents Program of the Chinese Academy of Sciences, Zhejiang Province Key Science and Technology Innovation Team (Grant No. 2013PT16), and Ningbo Natural Science Foundation (Grant No. 2015A610250). Yujing Bi thanks the scholarship of International Joint PhD Training Program sponsored by University of Chinese Academy of Sciences.

References

- 1 K. Xu, *Chem. Rev.*, 2004, **104**, 4303–4418.

- 2 S. Zhang, *J. Power Sources*, 2006, **162**, 1379–1394.
- 3 J. Vetter, P. Novak, M. R. Wagner, C. Veit, K.-C. Moller, J. O. Besenhard, M. Winter, M. Wohlfahrt-Mehrens, C. Vogler and A. Hammouche, *J. Power Sources*, 2005, **147**, 269–281.
- 4 D.-H. Cho, C.-H. Jo, W. Cho, Y.-J. Kim, H. Yashiro, Y.-K. Sun and S.-T. Myung, *J. Electrochem. Soc.*, 2014, **161**, A920–A926.
- 5 N. Tian, C. Hua, Z. Wang and L. Chen, *J. Mater. Chem. A*, 2015, **3**, 14173–14177.
- 6 K. Xu, *Chem. Rev.*, 2014, **114**, 11503–11618.
- 7 H. Kobayashi, M. Shikano, S. Koike, H. Sakaebe and K. Tatsumi, *J. Power Sources*, 2007, **174**, 380–386.
- 8 M. Shikano, H. Kobayashi, S. Koike, H. Sakaebe, E. Ikenaga, K. Kobayashi and K. Tatsumi, *J. Power Sources*, 2007, **174**, 795–799.
- 9 N. Takenaka, Y. Suzuki, H. Sakai and M. Nagaoka, *J. Phys. Chem. C*, 2014, **118**, 10874–10882.
- 10 R. Wang, X. Yu, J. Bai, H. Li, X. Huang, L. Chen and X. Yang, *J. Power Sources*, 2012, **218**, 113–118.
- 11 J. M. Garcia-Lastra, J. S. G. Myrdal, R. Christensen, K. S. Thygesen and T. Vegge, *J. Phys. Chem. C*, 2013, **117**, 5568–5577.
- 12 C. Ling, R. Zhang, K. Takechi and F. Mizuno, *J. Phys. Chem. C*, 2014, **118**, 26591–26598.
- 13 A. Manthiram, J. C. Knight, S.-T. Myung, S.-M. Oh and Y.-K. Sun, *Adv. Energy Mater.*, 2016, **6**, DOI: 10.1002/aenm.201501010.
- 14 W. Liu, P. Oh, X. Liu, M.-J. Lee, W. Cho, S. Chae, Y. Kim and J. Cho, *Angew. Chem., Int. Ed.*, 2015, **54**, 4440–4458.
- 15 G. V. Zhuang, G. Chen, J. Shim, X. Song, P. N. Ross and T. J. Richardson, *J. Power Sources*, 2004, **134**, 293–297.
- 16 Y. Bi, W. Yang, R. J. Zhou, M. Liu, Y. Liu and D. Wang, *J. Power Sources*, 2015, **283**, 211–218.
- 17 R. Du, Y. Bi, W. Yang, Z. Peng, M. Liu, Y. Liu, B. Wu, B. Yang, F. Ding and D. Wang, *Ceram. Int.*, 2015, **41**, 7133–7139.
- 18 R. Petibon, L. Madec, D. W. Abarbanel and J. R. Dahn, *J. Power Sources*, 2015, **300**, 419–429.
- 19 R. D. W. Kemmitt, D. R. Russell and D. W. A. Sharp, *J. Chem. Soc.*, 1963, **8**, 4408–4413.
- 20 J. G. Huddleston, A. E. Visser, W. M. Reichert, H. D. Willauer, G. A. Broker and R. Rogers, *Green Chem.*, 2001, **3**, 156–164.
- 21 L. Suo, O. Borodin, T. Gao, M. Olguin, J. Ho, X. Fan, C. Luo, C. Wang and K. Xu, *Science*, 2015, **350**, 938–943.
- 22 A. W. Cresce, M. Gobet, O. Borodin, J. Peng, S. M. Russell, E. Wikner, A. Fu, L. Hu, H.-S. Lee, Z. Zhang, X.-Q. Yang, S. Greenbaum, K. Amine and K. Xu, *J. Phys. Chem. C*, 2015, **119**, 27255–27264.
- 23 K. Xu and A. W. Cresce, *J. Mater. Res.*, 2012, **27**, 2327–2341.
- 24 A. W. Cresce and K. Xu, *Electrochem. Solid-State Lett.*, 2011, **14**, A154.
- 25 L. Madec, J. Xia, R. Petibon, K. J. Nelson, J.-P. Sun, I. G. Hill and J. R. Dahn, *J. Phys. Chem. C*, 2014, **118**, 29608–29622.
- 26 J. W. Diggle and A. Damjanovic, *J. Electrochem. Soc.*, 1972, **119**, 1649–1658.
- 27 R. Barnard, *J. Appl. Electrochem.*, 1973, **3**, 17–22.